

JEAN: Joint Expression and Audio-guided NeRF-based Talking Face Generation

Sai Tanmay Reddy Chakkerla
schakkerla@cs.stonybrook.edu

Stony Brook University
NY, USA

Aggelina Chatziagapi
aggelina@cs.stonybrook.edu

Dimitris Samaras
samaras@cs.stonybrook.edu

Abstract

We introduce a novel method for joint expression and audio-guided talking face generation. Recent approaches either struggle to preserve the speaker identity or fail to produce faithful facial expressions. To address these challenges, we propose a NeRF-based network. Since we train our network on monocular videos without any ground truth, it is essential to learn disentangled representations for audio and expression. We first learn audio features in a self-supervised manner, given utterances from multiple subjects. By incorporating a contrastive learning technique, we ensure that the learned audio features are aligned to the lip motion and disentangled from the muscle motion of the rest of the face. We then devise a transformer-based architecture that learns expression features, capturing long-range facial expressions and disentangling them from the speech-specific mouth movements. Through quantitative and qualitative evaluation, we demonstrate that our method can synthesize high-fidelity talking face videos, achieving state-of-the-art facial expression transfer along with lip synchronization to unseen audio. Project Page: <https://star52.github.io/publications/JEAN>

1 Introduction

Talking face generation has increasingly drawn attention due to its wide-ranging applications such as visual dubbing, video content creation and video conferencing. There are two main requirements in synthesizing a photorealistic talking face: (a) accurate lip synchronization to the spoken utterance, and (b) faithful facial expressions to convey a message with the intended affect. In human interaction, facial expressions deliver essential cues while talking [23, 24]. For example, the same sentence spoken with an angry or happy emotion can have a different meaning. Prior work has mostly focused on audio-only [16, 65, 80, 83, 98, 99] or expression-only [8, 9, 22, 45, 49, 66, 79] guidance for face synthesis. A few methods [41, 42, 43, 84] have tried to address the problem of simultaneous control of facial expressions and lips. However, they either struggle to preserve the speaker identity or fail to produce faithful expressions. Recently, neural radiance fields (NeRFs) [57] have demonstrated photorealistic 3D modeling, preserving identity-specific information and

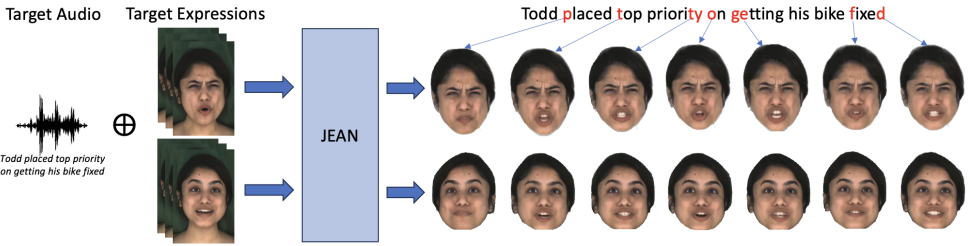


Figure 1: We introduce JEAN, a novel NeRF-based method that simultaneously combines lip-syncing to a target audio with facial expression transfer to generate talking faces.

faithfully reconstructing expressions [27]. However, NeRF-based methods have only addressed the problems of lip-syncing [12, 36, 51, 53, 95] or expression transfer [8, 6, 27, 61] separately.

In this work, we present JEAN, a novel **J**oint **E**xpression and **A**udio-guided NeRF for talking face generation. Our network is trained on monocular talking face videos without any ground truth. In these videos, the expression-related facial movements are strongly entangled with the speech-specific mouth movements. Controlling facial expressions and speech-specific lip motion separately requires learning *disentangled* representations for expression and audio correspondingly. To address this, we introduce a self-supervised approach to disentangle facial expressions from lip motion. We observe that mouth motion related to speech and face motion related to expressions in talking faces differ from each other temporally and spatially. Speech-related motion has higher temporal frequency and is spatially localized to the mouth region, while expression-related face motion has a lower temporal frequency and may occur over the entire face region. Moreover, for the same utterance spoken with different expressions, speech-related motion remains consistent. We leverage these observations to disentangle speech-related motion and expression-related motion.

We first learn a powerful audio representation in a self-supervised manner by disentangling the lip motion from the motion of the rest of the face in the feature space of an autoencoder. In general, achieving accurate lip synchronization on unseen audio in NeRFs is hard, as they tend to overfit on the training data [36]. Recently, contrastive learning has shown promise in synchronization in audio-visual tasks [63, 85, 89, 97]. This prompted us to introduce a contrastive learning strategy, in order to align the learned audio features with the lip motion. Next, we introduce a transformer-based architecture that learns expression features, capturing long-range facial expressions and disentangling them from speech-specific lip motion. Finally, we train a dynamic NeRF, conditioned on the learned representations for expression and audio. JEAN can synthesize high-fidelity talking face videos, faithfully following both the input facial expressions and speech signal for a given identity.

In brief, the contributions of our work are as follows:

- We introduce a self-supervised method to extract audio features aligned to lip motion features, achieving accurate lip synchronization on unseen audio.
- We propose a transformer-based module to learn expression features, disentangled from speech-specific mouth motion.
- Conditioning on the disentangled representations for expression and audio, we propose a novel NeRF-based method for simultaneous expression control and lip synchronization, outperforming the current state-of-the-art.

2 Related Work

Audio-driven Talking Face Generation. Audio-driven talking face generation aims to generate portrait images with synchronized lip motion to a given speech. Early attempts in talking face generation with lip synchronization [26, 47, 71] use probabilistic models to map speech phonemes to particular mouth shapes, requiring accurate annotation. More recent methods [13, 16, 65, 76, 80, 83, 97, 98, 99] learn neural networks, such as GANs, using a large amount of video data, containing multiple identities, in order to learn a robust audio-lip space. Our method, on the other hand, is NeRF-based, which enables us to better capture the 3D geometry and appearance of a talking face, and achieve higher output visual quality with just a few minutes of monocular video data.

NeRFs for Human Faces. Implicit neural representations for modeling 3D scenes have recently gained a lot of attention. In particular, neural radiance fields (NeRFs) [67] have shown photorealistic novel view synthesis of complex static [0, 8] and dynamic [62, 63, 67, 70] scenes. They represent a scene using an MLP, where each 3D point is associated with a radiance and density. Various recent works [27, 60, 61, 68, 75] use NeRFs to model the 3D face geometry. AD-NeRF [36] learns a dynamic NeRF conditioned on speech, encoded as DeepSpeech features [0, 32]. Follow-up methods [60, 61, 65, 72, 78, 93, 94, 95] enhance the lip synchronization in case of novel audio. NeRFace [27] conditions the network on 3DMM expression parameters. In contrast to the aforementioned approaches, our proposed NeRF allows for simultaneous control over facial expressions and lip motion to unseen audio.

Representation Learning for Human Faces. The task of representation learning for faces has been widely explored in unsupervised [14, 15, 21, 68, 46, 69, 88] and self-, semi-, or weakly-supervised [20, 60, 66, 70] techniques. In the talking face setting, where supervision is scarce and hard to find, self-supervision has been widely explored in the literature. Some methods have used self-supervision to improve the lip synchronization [63, 85, 93] in talking head generation tasks. Other methods have used self-supervised learning [29, 64, 82] to disentangle pose, expression, eye motion, etc., of a talking face to enable individual control. Other methods have used self-supervision to learn proxies, such as depth [69, 40], latent features [22] or keypoints [43] that improve generated talking faces. Our method disentangles expression from lip motion and aligns audio features to lip motion using self-supervision.

Expression and Audio-driven Talking Face Generation. Expression and audio-driven talking face generation aims to produce portrait images that follow expressions from an expression source and lips synchronized to an audio source. Prior work can be broadly classified into warping-based methods [43, 77] or synthesis-based methods [37, 41, 42, 64, 74, 74, 84]. Warping-based techniques estimate warping flows between source and target images, whereas synthesis-based methods generate images based on intermediate representations. Warping-based techniques, like EAMM [43], frequently produce 3D inconsistencies, since they consider only the 2D space. Synthesis-based methods, like PD-FGC [84], lead to the semantic leakage problem [70], where the output erroneously contains semantic elements of the input or training dataset. Some methods [62, 73, 74], such as EAT [28], learn a categorical emotional space, often based on one-hot encodings. In contrast, our method learns a NeRF controllable by both audio and expression from independent sources, giving 3D accurate and identity-preserved outputs with faithful expressions.

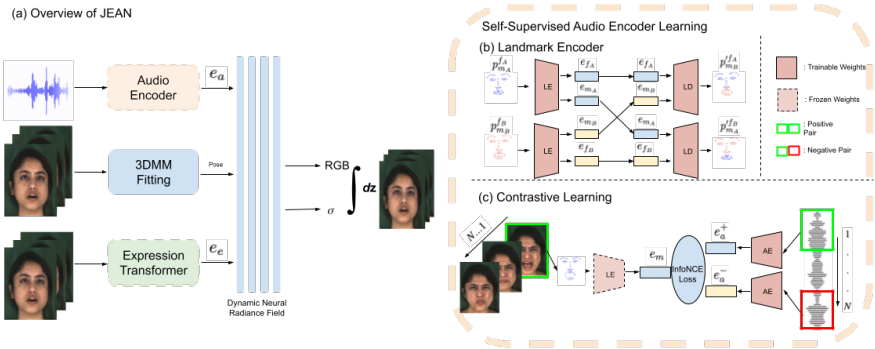


Figure 2: (a) illustrates an overview of JEAN, a novel method for joint expression and audio-guided NeRF-based talking face generation. (b) and (c) illustrate our proposed self-supervised learning of our audio representation. Specifically, (b) demonstrates the self-supervised learning of our landmark autoencoder that disentangles lip motion from the motion of the rest of the face. Then, in (c), our audio encoder AE is trained using a contrastive learning regime, in order to align audio features to lip motion.

3 Method

We present JEAN, a novel method for joint expression and audio-guided NeRF-based talking face generation. Fig. 2(a) illustrates an overview of our proposed approach. Given monocular RGB videos of an identity, we learn a NeRF that represents the identity’s 4D face geometry and appearance in various expressions and lip positions. We assume three inputs, namely an audio source, the identity’s head pose, and an expression source. During training, these inputs come from the same identity. During inference, we can use audio, pose, and expression sources from different videos. Our proposed pipeline consists of three main components: (1) We first learn an audio encoder in a self-supervised manner to align audio features to lip motion features (see Sec. 3.1). (2) We learn an expression transformer to disentangle expression features from lip motion (see Sec. 3.2). (3) Finally, we learn a dynamic NeRF conditioned on our learned representations for both audio and expression (see Sec. 3.3).

3.1 Self-Supervised Audio Encoder

In order to learn a powerful audio representation and achieve a high lip-sync accuracy, we propose a self-supervised contrastive learning method that aligns audio features to lip motion features. Inspired by Yao et al. [24], we first extract lip motion features through a landmark autoencoder. Next, we train our audio encoder using a contrastive learning strategy.

Landmark Autoencoder. We propose a landmark autoencoder that learns to disentangle mouth and eye-nose movements based on 2D landmarks, as illustrated in Fig. 2(b). For a frame A of an identity, we extract face landmarks $\mathbf{p}_{m_A}^{f_A}$, with superscript f_A indicating that the eye-nose landmarks are from frame A and subscript m_A indicating that mouth landmarks are from frame A . Similarly, for a frame B , we extract face landmarks $\mathbf{p}_{m_B}^{f_B}$. A landmark encoder (LE) embeds the input landmarks of each frame into an eye-nose embedding \mathbf{e}_f and a mouth embedding \mathbf{e}_m , i.e. $\mathbf{e}_{f_A}, \mathbf{e}_{m_A} = LE(\mathbf{p}_{m_A}^{f_A})$ and $\mathbf{e}_{f_B}, \mathbf{e}_{m_B} = LE(\mathbf{p}_{m_B}^{f_B})$. The mouth embeddings \mathbf{e}_{m_A} and \mathbf{e}_{m_B} of the two frames A and B correspondingly are swapped with a probability ϵ , and passed to a landmark decoder (LD) to predict the corresponding landmarks $\mathbf{p}_{m_B}^{f_A} =$

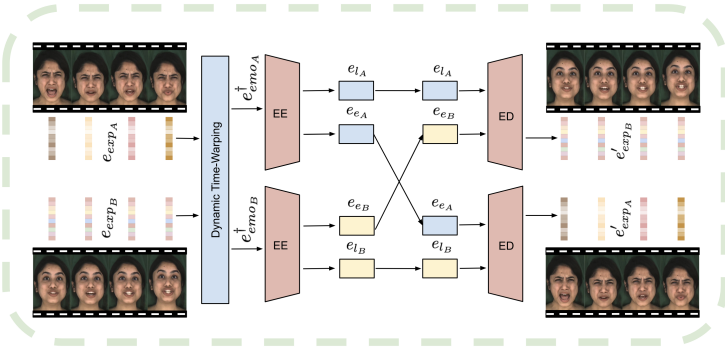


Figure 3: Expression Transformer. We propose an expression transformer encoder that learns to disentangle facial expressions from speech-specific lip motion. We extract emotion features and disentangle them into expression content and speech-specific lip motion content.

$LD(\mathbf{e}_{f_A}, \mathbf{e}_{m_B})$ and $\mathbf{p}_{m_A}^{f_B} = LD(\mathbf{e}_{f_B}, \mathbf{e}_{m_A})$. We get the ground truth $\mathbf{p}_{m_B}^{f_A}$ by replacing the mouth landmarks of the frame A with the corresponding mouth landmarks of the frame B . The autoencoder is trained using an L1 reconstruction loss:

$$\mathcal{L}_{rec_{lmd}} = \mathbf{E} \left[\|\mathbf{p}_{m_B}^{f_A} - \mathbf{p}_{m_B}^{f_A}\|_1 + \|\mathbf{p}_{m_A}^{f_B} - \mathbf{p}_{m_A}^{f_B}\|_1 \right]. \quad (1)$$

Using this training regime, the landmark encoder LE learns to represent the lip movements in its latent space, disentangling them from any other face motion. In our implementation, we extracted 68 face landmarks for each video frame. We discarded the first 17 landmarks that correspond to the face contour, in order to pay attention to the eye-nose and mouth movements. The probability ε is set to 0.8. The frames A and B are randomly sampled from the same video of an identity (see also suppl.).

Contrastive Learning. In order to learn audio embeddings aligned to the extracted mouth embeddings \mathbf{e}_m , we propose a contrastive training strategy, as illustrated in Fig. 2(c). We learn a CNN-based audio encoder AE that takes DeepSpeech [57] features \mathbf{a} as input and outputs audio embeddings \mathbf{e}_a , i.e. $\mathbf{e}_a = AE(\mathbf{a})$. For a mouth embedding \mathbf{e}_m , we set the corresponding audio feature \mathbf{e}_a^+ as the positive key and a randomly picked audio feature \mathbf{e}_a^- as the negative key. We train our audio encoder, using an InfoNCE [8] loss, to ensure that the distance between the positive pair $(\mathbf{e}_a^+, \mathbf{e}_m)$ is smaller than the negative one $(\mathbf{e}_a^-, \mathbf{e}_m)$:

$$\mathcal{L}_{\text{InfoNCE}} = - \mathbf{E}_{x \in \mathcal{X}} \left[\log \frac{\exp(d(\mathbf{e}_a^+, \mathbf{e}_{m_x}))}{\exp(d(\mathbf{e}_a^+, \mathbf{e}_{m_x})) + \exp(d(\mathbf{e}_a^-, \mathbf{e}_{m_x}))} \right], \quad (2)$$

where \mathcal{X} is the set of all $(\mathbf{e}_a^+, \mathbf{e}_m, \mathbf{e}_a^-)$ tuples and $d(\mathbf{x}, \mathbf{y}) = \frac{\langle \mathbf{x}, \mathbf{y} \rangle}{\tau \|\mathbf{x}\|_2 \|\mathbf{y}\|_2}$ is the temperature-adjusted cosine distance. During training, the negative audio samples are randomly selected from the same identity but different video. The temperature τ is set to 0.1. We use 64-dimensional features for \mathbf{e}_a , \mathbf{e}_f , and \mathbf{e}_m . See suppl. for more details.

3.2 Expression Transformer

We propose to learn an expression transformer that captures long-range facial expressions, disentangling them from the speech-specific lip motion (see Fig. 3). First, we extract emotion features e_{emo} per video frame, using a pre-trained network for emotion recognition [17].

We then learn an expression encoder that disentangles the emotion features into expression content and speech-specific content. The idea is that when a person is speaking, the face movements will have some aspects that are emotion-specific (e.g. cheeks pulled up, flush face, raised eyebrows, etc.) and some speech-specific (e.g. mouth motion for consonant ‘b’). Given that we have video pairs of a person saying the same utterance in different emotions, it is possible to capture the facial expressions and successfully disentangle them from the speech-specific motion. More specifically, for an utterance spoken with two different emotions A and B , we extract emotion features $\mathbf{e}_{emo_A[1:m_1]}$ and $\mathbf{e}_{emo_B[1:m_2]}$. We align these sequences, using the dynamic time warping (DTW) algorithm [9]:

$$\mathbf{e}_{emo_A[1:N]}^\dagger, \mathbf{e}_{emo_B[1:N]}^\dagger = DTW(\mathbf{e}_{emo_A[1:m_1]}, \mathbf{e}_{emo_B[1:m_2]}), \quad (3)$$

where m_1 and m_2 are the initial lengths and N is the output length of DTW. These are then given as input to the expression transformer encoder (EE) in windows of size ω . EE outputs expression features \mathbf{e}_e and speech-specific lip motion features \mathbf{e}_l , i.e. $\mathbf{e}_l[t : \omega + t - 1], \mathbf{e}_e[t : \omega + t - 1] = EE(\mathbf{e}_{emo[t:\omega+t-1]}^\dagger)$ where $t \in \mathbb{N}_{1:N}$. The expression features are randomly swapped with a probability δ . The output features \mathbf{e}_e and \mathbf{e}_l are input to the expression decoder (ED). ED follows an auto-regressive architecture to reconstruct the emotion features, i.e. $\mathbf{e}'_{emo[t:\omega+t-1]} = ED(\mathbf{e}_l[t : \omega + t - 1], \mathbf{e}_e[t : \omega + t - 1])$. The expression transformer is trained using an L1 reconstruction loss:

$$\mathcal{L}_{rec_{emo}} = \mathbf{E} [\|\mathbf{e}'_{emo_A} - \mathbf{e}_{emo_A}^\dagger\|_1 + \|\mathbf{e}'_{emo_B} - \mathbf{e}_{emo_B}^\dagger\|_1]. \quad (4)$$

During inference, DTW is skipped and the emotion features are directly input to EE . Our expression encoder is identity-specific, capturing each person’s unique way of speaking with a particular emotion. In our experiments, we set $\omega = 8$ and $\delta = 0.8$. EE and ED have 3 layers and 8 attention heads each. The emotion features e_{emo} are of 2048 dimension and mapped to 128 via 2 linear layers. The output of EE is split in half resulting in 64-dimensional $\mathbf{e}_l, \mathbf{e}_e$.

3.3 Dynamic NeRF

Our learned audio features \mathbf{e}_a and expression features \mathbf{e}_e are concatenated to an embedding \mathbf{e}_{in} , conditioning our dynamic NeRF that models the 4D face dynamics of a subject. For each video frame, we fit a 3DMM [11, 52] and extract the head pose and camera parameters, in order to estimate the viewing direction \mathbf{d} . The learned feature \mathbf{e}_{in} , the viewing direction \mathbf{d} and a 3D point location \mathbf{x} in canonical space are input to the implicit function F_Θ (MLP), which predicts the corresponding RGB color \mathbf{c} and density σ :

$$F_\Theta : (\mathbf{e}_{in}, \mathbf{d}, \mathbf{x}) \longrightarrow (\mathbf{c}, \sigma) \quad (5)$$

Given the color \mathbf{c} and density σ at each sampled point of every ray, we can reconstruct each video frame using volumetric rendering. For each camera ray $\mathbf{r}(t) = \mathbf{o} + t\mathbf{d}$, where \mathbf{o} is the camera center, the color C is estimated by accumulating the RGB colors and densities of the points sampled along the ray: $C(\mathbf{r}; \Theta) = \int_{t_n}^{t_f} \sigma_\Theta(\mathbf{r}(t)) \mathbf{c}_\Theta(\mathbf{r}(t), \mathbf{d}) T(t) dt$ [57], where $T(s) = \exp(-\int_{t_n}^s \sigma_\Theta(\mathbf{r}(s)) ds)$ is the accumulated transmittance from t_n to t , and t_f and t_n are the far and near bounds respectively. We denote the outputs of F_Θ as \mathbf{c}_Θ and σ_Θ for brevity. Similar to [57], we learn a coarse and a fine model for hierarchical volumetric rendering. We optimize our NeRF using a photo-consistency loss:

$$\mathcal{L}_{photo} = \sum_{\mathbf{r} \in \mathcal{R}} \|\hat{C}(\mathbf{r}; \Theta) - C(\mathbf{r}; \Theta)\|_2^2, \quad (6)$$

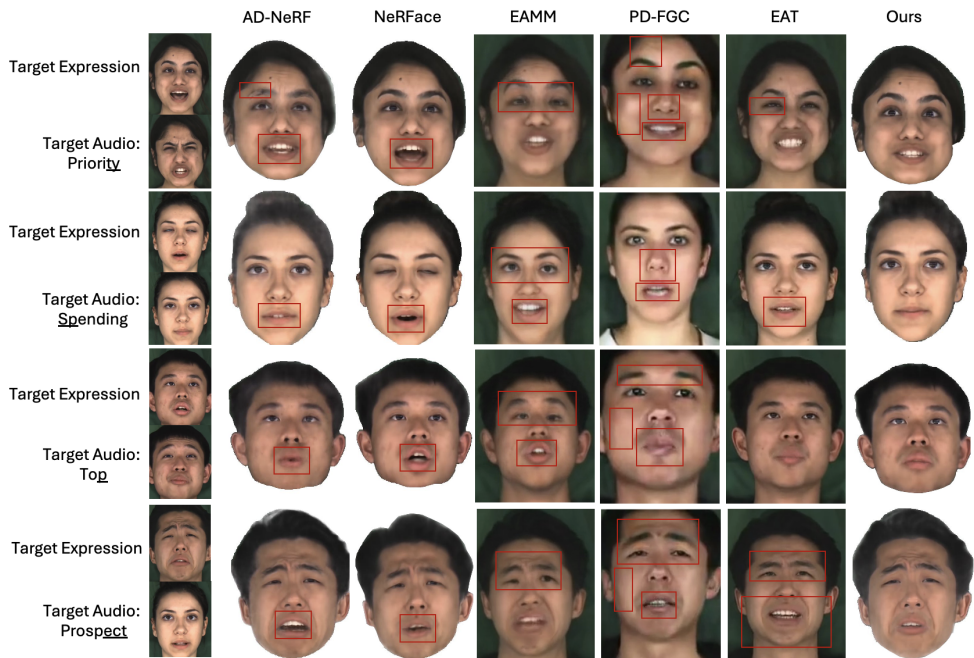


Figure 4: Talking face generation guided by target expression and audio sources (1st column). We compare with state-of-the-art methods for expression and audio-driven talking face generation (EAMM [13], PD-FGC [24]), categorical emotion based talking face generation (EAT [28]), as well as the audio-only AD-NeRF [67], and expression-only NeRFace [17]. Our method outperforms all these methods, transferring the expression and audio inputs with higher fidelity, while preserving the target identity.

which measures the mean squared error between the ground truth color $C(\mathbf{r}; \Theta)$ and the predicted color $\hat{C}(\mathbf{r}; \Theta)$, and \mathcal{R} is the set of all the rays in each batch (see also suppl.).

4 Experiments

Dataset. In our experiments, we use the MEAD dataset [66]. MEAD includes 48 identities, performing 7 emotions at 3 intensity levels and 1 neutral emotion. The videos are captured by 7 cameras at different viewpoints. Each emotion level contains $\approx 30 - 40$ videos corresponding to an utterance sampled from a superset of sentences. To train our audio encoder (see Sec. 3.1), we use the complete set of frontal-view videos. For the expression transformer (see Sec. 3.2), we need video pairs, where a person pronounces the same utterance with different emotions. We use the highest level (level 3) of the emotions “angry”, “happy” and “sad”, and the single level of “neutral”, leading to a total of 84 unique pairs of sentences being spoken in 2 emotions. Of those, 60 pairs of videos are used for training, and 24 for validation. Since each person’s expressions are unique, we train an expression transformer for each identity. To train our dynamic NeRF, we focus on 4 identities from MEAD, training the network for each identity. Since the videos in MEAD are only 4-8 seconds long, we concatenate videos of the same emotion for each identity. Not all the videos of the same emotion for an identity were captured in the same head pose, so we filter videos based on the

Table 1: Quantitative comparison of our method with the state-of-the-art. Results are highlighted as follows: **Best**, **Second Best** and **Third Best**.

Method	LSE-C \uparrow	ACD \downarrow	Exp-Diff \downarrow	PSNR \uparrow	SSIM \uparrow	LPIPS \downarrow
AD-NeRF [66]	4.380	0.141	0.080	20.467	0.698	0.187
NeRFace [27]	1.966	0.103	0.023	21.335	0.736	0.175
EAMM [43]	1.771	0.284	0.111	18.474	0.592	0.248
PD-FGC [82]	6.220	0.657	0.089	21.094	0.648	0.228
EAT [28]	7.200	0.183	0.078	19.222	0.691	0.205
Ours	4.466	0.095	0.043	21.224	0.720	0.174

estimated focal length and the pose distribution after fitting a 3DMM. After concatenation, we get videos of at least 12 seconds per emotion. See suppl. for more details.

4.1 Results

In this section, we compare our proposed method with the state-of-the-art. We include comparisons with AD-NeRF [66] that takes only audio as input and NeRFace [27] that takes only 3DMM expression parameters as input, in order to illustrate our method’s performance against NeRF-based methods with just one of the inputs, audio or expression. Then, we compare with EAMM [43], PD-FGC [82], and EAT [28] that are identity-generic methods for emotion-aware talking face video generation, trained on large datasets. Note that while EAMM and PD-FGC use a video source for expressions, EAT only takes an emotion label as input to produce expressions. Our method achieves the best disentanglement between expression and audio sources, producing high-quality expressive talking faces.

4.1.1 Qualitative Evaluation

Fig. 4 shows our qualitative results. Notice how our method produces accurate lip shapes that follow the target audio (*e.g.* phoneme “t” in row 2), while also synthesizing the input expression (*e.g.* sad) with higher fidelity than the other methods. EAMM generally distorts the input face, adds asymmetrical artifacts, and is unable to produce accurate mouth shapes in all rows. While PD-FGC performs better than EAMM in terms of lip-shape accuracy, it still distorts the input identity and produces artifacts. For example, we observe glossy faces, color distortions and lip artifacts in all rows, a plain white band in place of teeth in rows 1 and 2, and loss of identity-specific characteristics, such as the mole on the face of the woman in row 1. EAT performs best among the other methods, creating accurate lip shapes, synced to the input audio, while also being faithful to the source emotions. However, EAT still struggles with preserving the input identity. For example, it generates artifacts in the eye region and eyebrows in rows 1 and 4 respectively, and wide jaws and crossed eyes in row 4. In general, we observe identity inconsistency problems in all EAMM, PD-FGC, and EAT. In contrast, the NeRF-based methods, *i.e.* AD-NeRF, NeRFace, and our method, learn to preserve the input identity. Our method demonstrates high-quality results, transferring the source facial expression and following the source audio with higher fidelity.

4.1.2 Quantitative Evaluation

Evaluation Metrics. We conduct quantitative evaluation on common metrics used in the talking face generation field. We use LSE-C [65] to measure the lip synchronization of

Table 2: Ablation study on our proposed audio and expression representations. In (a), we train the network without the self-supervised audio encoder learning and without expression transformer (we use features from the pre-trained ResNet-based emotion recognition network from [17] passed through a thin MLP). In (b), we again omit the self-supervised audio encoder learning and use 3DMM expression parameters. In (c), we add the self-supervised audio encoder learning, but we use expression features as in (a). In (d), we train our expression transformer on 3DMM expression parameters. Best results are highlighted in **bold**.

Variant	Method					Metrics		
	Self Super-vised Audio Encoder	3DMM Ex-pression Pa-rameters	Emotion Recognition Features	Expression Transformer		LSE-C \uparrow	Exp-Diff \downarrow	LPIPS \downarrow
(a)				✓		1.804	0.027	0.170
(b)		✓				1.848	0.022	0.161
(c)	✓			✓		1.760	0.028	0.168
(d)	✓	✓			✓	2.982	0.071	0.190
Full Net.	✓			✓	✓	4.466	0.043	0.174

our method, and Peak Signal-to-Noise Ratio (PSNR), Structural Similarity (SSIM) [87] and Learned Perceptual Image Patch Similarity (LPIPS) [96] to measure the image quality against the expression source images. We also estimate the expression transfer accuracy (Exp-Diff) [84] by using 3D face reconstruction [19] and calculating the Mean Squared Error (MSE) of the extracted expression parameters in the synthesized images with those of the driving expression images. Further, we estimate the identity preservation using the Average Content Distance (ACD) metric, inspired by [83], by calculating the cosine distance between ArcFace [18] face recognition embeddings of synthesized images and driving expression images. Essentially, the idea is that the smaller the distance between those embeddings, the closer are the synthesized images to the driving images in terms of identity.

We show the corresponding quantitative results in Table 1. Since Exp-Diff and the visual quality metrics are computed against expression source frames, we find that the expression-only NeRFace performs best on those metrics. Our method significantly outperforms the state-of-the-art in emotion-aware talking face generation (EAMM, PD-FGC, EAT) in terms of visual quality (PSNR, SSIM, LPIPS), identity preservation (ACD), and expression transfer (Exp-Diff). While PD-FGC and EAT do perform better than our method in terms of lip-syncing, as they are trained on large-scale video data, our method outperforms the rest of the methods. We encourage the readers to watch our suppl. video for additional results demonstrating the efficacy of JEAN.

4.1.3 Ablation Study

Expression Disentanglement. Table 2 shows different variants of our method, demonstrating the efficacy of our self-supervised learning of our audio representation, as well as the disentanglement of our expression representation. More specifically, in variant (a), we omit the self-supervised audio encoder learning and the expression transformer (we directly use features from a pre-trained ResNet-based emotion recognition network from [17] mapped through a thin MLP, and the audio encoder is trained along with the NeRF). In variant (b), we use 3DMM [62] expression parameters and skip the self-supervised audio encoder. In variant (c), we add the self-supervised audio encoder learning, but we use expression features as in (a). Finally, in variant (d), we learn the expression features, using 3DMM expression pa-



Figure 5: Additional analysis that shows that the expression encoder disentangles features that are semantically grounded and well-behaved. Interpolation of features between different emotional expressions leads to semantically meaningful expressions.

rameters as input to our transformer. We see that not disentangling the emotion recognition features in (a) and (c), and the expression parameters from [14, 62] in (b), cause the NeRF network to only learn expressions from the expression source and ignore the audio source. This leads to a significant decrease in lip-sync metrics on unseen audio and best performance in terms of Exp-Diff and LPIPS. Further, trying to disentangle 3DMM expression parameters in (d) fails to learn meaningful features which leads to poor lip-sync metrics on unseen audio and the worst performance in terms of Exp-Diff and LPIPS. Our proposed expression transformer leads to a successful disentanglement between expression and speech-specific lip motion. Note that Exp-Diff is computed against the driving expression images, which implies that if the network has overfitted to the driving expression the corresponding Exp-Diff would also be lower. Disentangling expressions from lip motion leads to a balanced performance between expression and lip-sync accuracy.

Interpreting Learnt Features. In Fig. 5, we conduct further analysis to investigate the proposed expression disentanglement and the nature of the learned expression features. The interpolation result between two expression features, learned by our expression transformer, shows that our method learns semantically grounded features. In the suppl. material, we show additional interpolation results and show t-SNE plots of the learned expression features, indicating that they are semantically meaningful.

5 Conclusion

In conclusion, we introduce a novel method for joint expression and audio-guided talking face generation. Prior work either struggles to preserve the speaker identity or fails to synthesize faithful facial expressions. We propose a self-supervised method to extract audio features, aligned to lip motion, achieving accurate lip synchronization to unseen audio. In addition, we design a transformer-based module to learn expression features, disentangled from speech-specific mouth motion. By conditioning on the learned representations, our dynamic NeRF synthesizes high-fidelity talking face videos, providing simultaneous control of facial expressions and lip movements, and outperforming the current state-of-the-art. We argue that our proposed representations can be easily extended to other neural rendering pipelines, such as Gaussian Splatting [44], that we plan to explore as future work.

Acknowledgements. This work was supported in part by Amazon Prime Video and a grant from the CDC/NIOSH (U01 OH012476).

References

- [1] Chaitanya Ahuja, Dong Won Lee, Yukiko I. Nakano, and Louis-Philippe Morency. Style transfer for co-speech gesture animation: A multi-speaker conditional-mixture approach. In *Eur. Conf. Comput. Vis.*, 2020.
- [2] Dario Amodei, Sundaram Ananthanarayanan, Rishita Anubhai, Jingliang Bai, Eric Battenberg, Carl Case, Jared Casper, Bryan Catanzaro, Qiang Cheng, Guoliang Chen, Jie Chen, Jingdong Chen, Zhijie Chen, Mike Chrzanowski, Adam Coates, Greg Diamos, Ke Ding, Niandong Du, Erich Elsen, Jesse Engel, Weiwei Fang, Linxi Fan, Christopher Fougner, Liang Gao, Caixia Gong, Awni Hannun, Tony Han, Lappi Vaino Johannes, Bing Jiang, Cai Ju, Billy Jun, Patrick LeGresley, Libby Lin, Junjie Liu, Yang Liu, Weigao Li, Xiangang Li, Dongpeng Ma, Sharan Narang, Andrew Ng, Sherjil Ozair, Yiping Peng, Ryan Prenger, Sheng Qian, Zongfeng Quan, Jonathan Raiman, Vinay Rao, Sanjeev Satheesh, David Seetapun, Shubho Sengupta, Kavya Srinet, Anuroop Sriram, Haiyuan Tang, Liliang Tang, Chong Wang, Jidong Wang, Kaifu Wang, Yi Wang, Zhijian Wang, Zhiqian Wang, Shuang Wu, Likai Wei, Bo Xiao, Wen Xie, Yan Xie, Dani Yogatama, Bin Yuan, Jun Zhan, and Zhenyao Zhu. Deep speech 2: end-to-end speech recognition in english and mandarin. In *Int. Conf. Mach. Learn.*, 2016.
- [3] ShahRukh Athar, Zhixin Shu, and Dimitris Samaras. Self-supervised deformation modeling for facial expression editing. In *IEEE Conf. Face Gest. Recog. (FG)*, 2019.
- [4] ShahRukh Athar, Albert Pumarola, Francesc Moreno-Noguer, and Dimitris Samaras. Facedet3d: Facial expressions with 3d geometric detail prediction. *ArXiv*, abs/2012.07999, 2020.
- [5] ShahRukh Athar, Zexiang Xu, Kalyan Sunkavalli, Eli Shechtman, and Zhixin Shu. Rignerf: Fully controllable neural 3d portraits. In *IEEE Conf. Comput. Vis. Pattern Recog.*, 2022.
- [6] ShahRukh Athar, Zhixin Shu, and Dimitris Samaras. Flame-in-nerf: Neural control of radiance fields for free view face animation. In *IEEE Conf. Face Gest. Recog. (FG)*, 2023.
- [7] Jonathan T Barron, Ben Mildenhall, Matthew Tancik, Peter Hedman, Ricardo Martin-Brualla, and Pratul P Srinivasan. Mip-nerf: A multiscale representation for anti-aliasing neural radiance fields. In *Int. Conf. Comput. Vis.*, 2021.
- [8] Jonathan T Barron, Ben Mildenhall, Dor Verbin, Pratul P Srinivasan, and Peter Hedman. Mip-nerf 360: Unbounded anti-aliased neural radiance fields. In *IEEE Conf. Comput. Vis. Pattern Recog.*, 2022.
- [9] R. Bellman and R. Kalaba. On adaptive control processes. *IRE Transactions on Automatic Control*, 4(2):1–9, 1959.
- [10] Zhixi Cai, Shreya Ghosh, Kalin Stefanov, Abhinav Dhall, Jianfei Cai, Hamid Rezatofighi, Reza Haffari, and Munawar Hayat. Marlin: Masked autoencoder for facial video representation learning. In *IEEE Conf. Comput. Vis. Pattern Recog.*, 2023.

- [11] Chen Cao, Yanlin Weng, Shun Zhou, Yiyong Tong, and Kun Zhou. Facewarehouse: A 3d facial expression database for visual computing. *IEEE Trans. Vis. Comput. Graph.*, 20(3):413–425, 2013.
- [12] Aggelina Chatziagapi, ShahRukh Athar, Abhinav Jain, Rohith MV, Vimal Bhat, and Dimitris Samaras. Lipnerf: What is the right feature space to lip-sync a nerf? In *IEEE Conf. Face Gest. Recog. (FG)*, 2023.
- [13] Lele Chen, Ross K. Maddox, Zhiyao Duan, and Chenliang Xu. Hierarchical cross-modal talking face generation with dynamic pixel-wise loss. In *IEEE Conf. Comput. Vis. Pattern Recog.*, 2019.
- [14] Ricky TQ Chen, Xuechen Li, Roger B Grosse, and David K Duvenaud. Isolating sources of disentanglement in variational autoencoders. In *Adv. Neural Inform. Process. Syst.*, 2018.
- [15] Xi Chen, Yan Duan, Rein Houthoofd, John Schulman, Ilya Sutskever, and Pieter Abbeel. Infogan: Interpretable representation learning by information maximizing generative adversarial nets. In *Adv. Neural Inform. Process. Syst.*, 2016.
- [16] JS Chung, A Jamaludin, A Zisserman, et al. You said that? In *Brit. Mach. Vis. Conf.*, 2017.
- [17] Radek Danecek, Michael J. Black, and Timo Bolkart. EMOCA: Emotion driven monocular face capture and animation. In *IEEE Conf. Comput. Vis. Pattern Recog.*, 2022.
- [18] Jiankang Deng, Jia Guo, Niannan Xue, and Stefanos Zafeiriou. Arcface: Additive angular margin loss for deep face recognition. In *IEEE Conf. Comput. Vis. Pattern Recog.*, 2019.
- [19] Yu Deng, Jiaolong Yang, Sicheng Xu, Dong Chen, Yunde Jia, and Xin Tong. Accurate 3d face reconstruction with weakly-supervised learning: From single image to image set. In *IEEE Conf. Comput. Vis. Pattern Recog. Worksh.*, 2019.
- [20] Yu Deng, Jiaolong Yang, Dong Chen, Fang Wen, and Xin Tong. Disentangled and controllable face image generation via 3d imitative-contrastive learning. In *IEEE Conf. Comput. Vis. Pattern Recog.*, 2020.
- [21] Zheng Ding, Yifan Xu, Weijian Xu, Gaurav Parmar, Yang Yang, Max Welling, and Zhuowen Tu. Guided variational autoencoder for disentanglement learning. In *IEEE Conf. Comput. Vis. Pattern Recog.*, 2020.
- [22] Michail Christos Doukas, Mohammad Rami Koujan, Viktoriia Sharmanska, Anastasios Roussos, and Stefanos Zafeiriou. Head2head++: Deep facial attributes re-targeting. *IEEE Trans. Bio., Beh., Id. Sci.*, 3:31–43, 2020.
- [23] Paul Ekman and Wallace V. Friesen. Facial action coding system: a technique for the measurement of facial movement. *Environmental Psychology and Nonverbal Behavior*, 1978.

- [24] Paul Ekman and Erika L. Rosenberg. *What the Face Reveals: Basic and Applied Studies of Spontaneous Expression Using the Facial Action Coding System (FACS)*. Oxford University Press, 04 2005.
- [25] William Fedus, Ian Goodfellow, and Andrew M. Dai. MaskGAN: Better text generation via filling in the _____. In *Int. Conf. Learn. Represent.*, 2018.
- [26] Shengli Fu, R. Gutierrez-Osuna, A. Esposito, P.K. Kakumanu, and O.N. Garcia. Audio/visual mapping with cross-modal hidden markov models. *IEEE Trans. Multimedia*, 7(2):243–252, 2005.
- [27] Guy Gafni, Justus Thies, Michael Zollhöfer, and Matthias Nießner. Dynamic neural radiance fields for monocular 4d facial avatar reconstruction. In *IEEE Conf. Comput. Vis. Pattern Recog.*, 2021.
- [28] Yuan Gan, Zongxin Yang, Xihang Yue, Lingyun Sun, and Yi Yang. Efficient emotional adaptation for audio-driven talking-head generation. In *Int. Conf. Comput. Vis.*, 2023.
- [29] Yue Gao, Yuan Zhou, Jinglu Wang, Xiao Li, Xiang Ming, and Yan Lu. High-fidelity and freely controllable talking head video generation. In *IEEE Conf. Comput. Vis. Pattern Recog.*, 2023.
- [30] Partha Ghosh, Pravir Singh Gupta, Roy Uziel, Anurag Ranjan, Michael J. Black, and Timo Bolkart. Gif: Generative interpretable faces. In *IEEE Conf. 3D Vis. (3DV)*, 2020.
- [31] Shiry Ginosar, Amir Bar, Gefen Kohavi, Caroline Chan, Andrew Owens, and Jitendra Malik. Learning individual styles of conversational gesture. In *IEEE Conf. Comput. Vis. Pattern Recog.*, 2019.
- [32] Sahil Goyal, Sarthak Bhagat, Shagun Uppal, Hitkul Jangra, Yi Yu, Yifang Yin, and Rajiv Ratn Shah. Emotionally enhanced talking face generation. In *Int. Conf. Multimedia Workshop*, 2023.
- [33] Jia Guo, Jiankang Deng, Xiang An, Jack Yu, and Baris Gecer. Insightface repository model zoo. URL https://github.com/deepinsight/insightface/tree/master/model_zoo.
- [34] Jianzhu Guo, Xiangyu Zhu, and Zhen Lei. 3ddfa. <https://github.com/clearidusk/3DDFA>, 2018.
- [35] Jianzhu Guo, Xiangyu Zhu, Yang Yang, Fan Yang, Zhen Lei, and Stan Z Li. Towards fast, accurate and stable 3d dense face alignment. In *Eur. Conf. Comput. Vis.*, 2020.
- [36] Yudong Guo, Keyu Chen, Sen Liang, Yongjin Liu, Hujun Bao, and Juyong Zhang. Ad-nerf: Audio driven neural radiance fields for talking head synthesis. In *Int. Conf. Comput. Vis.*, 2021.
- [37] Awni Hannun, Carl Case, Jared Casper, Bryan Catanzaro, Greg Diamos, Erich Elsen, Ryan Prenger, Sanjeev Satheesh, Shubho Sengupta, Adam Coates, and Andrew Y. Ng. Deep speech: Scaling up end-to-end speech recognition. *arXiv:1412.5567*, 2014.

- [38] Irina Higgins, Loic Matthey, Arka Pal, Christopher P Burgess, Xavier Glorot, Matthew M Botvinick, Shakir Mohamed, and Alexander Lerchner. beta-vae: Learning basic visual concepts with a constrained variational framework. In *Int. Conf. Learn. Represent.*, 2017.
- [39] Fa-Ting Hong, Longhao Zhang, Li Shen, and Dan Xu. Depth-aware generative adversarial network for talking head video generation. In *IEEE Conf. Comput. Vis. Pattern Recog.*, 2022.
- [40] Fa-Ting Hong, , Li Shen, and Dan Xu. Dagan++: Depth-aware generative adversarial network for talking head video generation. *IEEE Trans. Pattern Anal. Mach. Intell.*, 46(5):2997–3012, 2023.
- [41] Youngjoon Jang, Kyeongha Rho, Jongbin Woo, Hyeongkeun Lee, Jihwan Park, Youshin Lim, Byeong-Yeol Kim, and Joon Son Chung. That’s what i said: Fully-controllable talking face generation. In *ACM Int. Conf. Multimedia*, 2023.
- [42] Xinya Ji, Hang Zhou, Kaisiyuan Wang, Wayne Wu, Chen Change Loy, Xun Cao, and Feng Xu. Audio-driven emotional video portraits. In *IEEE Conf. Comput. Vis. Pattern Recog.*, 2021.
- [43] Xinya Ji, Hang Zhou, Kaisiyuan Wang, Qianyi Wu, Wayne Wu, Feng Xu, and Xun Cao. Eamm: One-shot emotional talking face via audio-based emotion-aware motion model. In *ACM Proc. SIGGRAPH*, 2022.
- [44] Bernhard Kerbl, Georgios Kopanas, Thomas Leimkühler, and George Drettakis. 3d gaussian splatting for real-time radiance field rendering. *ACM Trans. Graph.*, 42(4), 2023.
- [45] Hyeongwoo Kim, Pablo Garrido, Ayush Tewari, Weipeng Xu, Justus Thies, Matthias Nießner, Patrick Pérez, Christian Richardt, Michael Zollöfer, and Christian Theobalt. Deep video portraits. *ACM Trans. Graph.*, 37(4):163, 2018.
- [46] Hyunjik Kim and Andriy Mnih. Disentangling by factorising. In *Int. Conf. Mach. Learn.*, 2018.
- [47] Taehwan Kim, Yisong Yue, Sarah Taylor, and Iain Matthews. A decision tree framework for spatiotemporal sequence prediction. In *Proc. ACM SIGKDD Int. Conf. Knowledge Disc. Data Mining*, 2015.
- [48] Diederik P Kingma and Jimmy Ba. Adam: a method for stochastic optimization. In *Int. Conf. Learn. Represent.*, 2014.
- [49] Mohammad Rami Koujan, Michail Christos Doukas, Anastasios Roussos, and Stefanos Zafeiriou. Head2head: Video-based neural head synthesis. In *IEEE Conf. Face Gest. Recog. (FG)*, 2020.
- [50] Dongze Li, Kang Zhao, Wei Wang, Bo Peng, Yingya Zhang, Jing Dong, and Tieniu Tan. Ae-nerf: Audio enhanced neural radiance field for few shot talking head synthesis. *Proc. AAAI Conf. on Art. Intel.*, 38(4), 2024.

- [51] Jiahe Li, Jiawei Zhang, Xiao Bai, Jun Zhou, and Lin Gu. Efficient region-aware neural radiance fields for high-fidelity talking portrait synthesis. In *Int. Conf. Comput. Vis.*, 2023.
- [52] Tianye Li, Mira Slavcheva, Michael Zollhöfer, Simon Green, Christoph Lassner, Changil Kim, Tanner Schmidt, Steven Lovegrove, Michael Goesele, Richard Newcombe, and Zhaoyang Lv. Neural 3d video synthesis from multi-view video. In *IEEE Conf. Comput. Vis. Pattern Recog.*, 2022.
- [53] Zhengqi Li, Simon Niklaus, Noah Snavely, and Oliver Wang. Neural scene flow fields for space-time view synthesis of dynamic scenes. In *IEEE Conf. Comput. Vis. Pattern Recog.*, 2021.
- [54] Jiyuan Liu, Wenping Wei, Zhendong Li, Guanfeng Li, and Hao Liu. Invariant motion representation learning for 3d talking face synthesis. In *ICASSP*, 2024.
- [55] Xian Liu, Yinghao Xu, Qianyi Wu, Hang Zhou, Wayne Wu, and Bolei Zhou. Semantic-aware implicit neural audio-driven video portrait generation. In *Eur. Conf. Comput. Vis.*, 2022.
- [56] Yuanxun Lu, Jinxiang Chai, and Xun Cao. Live speech portraits: real-time photorealistic talking-head animation. *ACM Trans. Graph.*, 40(6), 2021.
- [57] Ben Mildenhall, Pratul P. Srinivasan, Matthew Tancik, Jonathan T. Barron, Ravi Ramamoorthi, and Ren Ng. Nerf: Representing scenes as neural radiance fields for view synthesis. In *Eur. Conf. Comput. Vis.*, 2020.
- [58] Ali Mollahosseini, Behzad Hasani, and Mohammad H. Mahoor. Affectnet: A database for facial expression, valence, and arousal computing in the wild. *IEEE Trans. Affect. Comput.*, 10(1):18–31, 2019.
- [59] Thu Nguyen-Phuoc, Chuan Li, Lucas Theis, Christian Richardt, and Yong-Liang Yang. Hologan: Unsupervised learning of 3d representations from natural images. In *IEEE Conf. Comput. Vis. Pattern Recog.*, 2019.
- [60] Keunhong Park, Utkarsh Sinha, Jonathan T. Barron, Sofien Bouaziz, Dan B Goldman, Steven M. Seitz, and Ricardo Martin-Brualla. Nerfies: Deformable neural radiance fields. In *Int. Conf. Comput. Vis.*, 2021.
- [61] Keunhong Park, Utkarsh Sinha, Peter Hedman, Jonathan T. Barron, Sofien Bouaziz, Dan B Goldman, Ricardo Martin-Brualla, and Steven M. Seitz. Hypernerf: A higher-dimensional representation for topologically varying neural radiance fields. *ACM Trans. Graph.*, 40(6), 2021.
- [62] Pascal Paysan, Reinhard Knothe, Brian Amberg, Sami Romdhani, and Thomas Vetter. A 3d face model for pose and illumination invariant face recognition. In *2009 Sixth IEEE International Conference on Advanced Video and Signal Based Surveillance*, 2009.
- [63] Ziqiao Peng, Yihao Luo, Yue Shi, Hao Xu, Xiangyu Zhu, Hongyan Liu, Jun He, and Zhaoxin Fan. Selftalk: A self-supervised commutative training diagram to comprehend 3d talking faces. In *ACM Int. Conf. Multimedia*, 2023.

- [64] Ziqiao Peng, Wentao Hu, Yue Shi, Xiangyu Zhu, Xiaomei Zhang, Hao Zhao, Jun He, Hongyan Liu, and Zhaoxin Fan. Synctalk: The devil is in the synchronization for talking head synthesis. In *IEEE Conf. Comput. Vis. Pattern Recog.*, 2024.
- [65] K R Prajwal, Rudrabha Mukhopadhyay, Vinay P. Namboodiri, and C.V. Jawahar. A lip sync expert is all you need for speech to lip generation in the wild. In *ACM Int. Conf. Multimedia*, 2020.
- [66] Albert Pumarola, Antonio Agudo, Aleix M Martinez, Alberto Sanfeliu, and Francesc Moreno-Noguer. Ganimation: Anatomically-aware facial animation from a single image. In *Eur. Conf. Comput. Vis.*, 2018.
- [67] Albert Pumarola, Enric Corona, Gerard Pons-Moll, and Francesc Moreno-Noguer. D-nerf: Neural radiance fields for dynamic scenes. In *IEEE Conf. Comput. Vis. Pattern Recog.*, 2021.
- [68] Amit Raj, Michael Zollhoefer, Tomas Simon, Jason Saragih, Shunsuke Saito, James Hays, and Stephen Lombardi. Pva: Pixel-aligned volumetric avatars. In *arXiv:2101.02697*, 2020.
- [69] Tal Reiss, Bar Cavia, and Yedid Hoshen. Detecting deepfakes without seeing any. *arXiv preprint arXiv:2311.01458*, 2023.
- [70] Yurui Ren, Gezhong Li, Yuanqi Chen, Thomas H. Li, and Shan Liu. Pirenderer: Controllable portrait image generation via semantic neural rendering. In *Int. Conf. Comput. Vis.*, 2021.
- [71] Shinji Sako, Keiichi Tokuda, Takashi Masuko, Takao Kobayashi, and Tadashi Kitamura. Hmm-based text-to-audio-visual speech synthesis. In "*Proc. Int. Speech Comm. Assn., INTERSPEECH*", 2000.
- [72] Shuai Shen, Wanhua Li, Xiaoke Huang, Zheng Zhu, Jie Zhou, and Jiwen Lu. Sd-nerf: Towards lifelike talking head animation via spatially-adaptive dual-driven nerfs. *IEEE Trans. Multimedia*, 26:3221–3234, 2024.
- [73] Zhicheng Sheng, Liqiang Nie, Min Zhang, Xiaojun Chang, and Yan Yan. Stochastic latent talking face generation toward emotional expressions and head poses. *IEEE Trans. Cir. Sys. Vid. Tech.*, 34(4):2734–2748, 2024.
- [74] Sanjana Sinha, S. Biswas, Ravindra Yadav, and B. Bhowmick. Emotion-controllable generalized talking face generation. In *IJCAI*, 2022.
- [75] Tiancheng Sun, Kai-En Lin, Sai Bi, Zexiang Xu, and Ravi Ramamoorthi. Nelf: Neural light-transport field for portrait view synthesis and relighting. In *Eurographics Symposium on Rendering*, 2021.
- [76] Supasorn Suwajanakorn, Steven M. Seitz, and Ira Kemelmacher-Shlizerman. Synthesizing obama: learning lip sync from audio. *ACM Trans. Graph.*, 36(4):1–13, 2017.
- [77] Shuai Tan, Bin Ji, and Ye Pan. Emnm: Emotional motion memory network for audio-driven emotional talking face generation. In *Int. Conf. Comput. Vis.*, 2023.

- [78] Jiaxiang Tang, Kaisiyuan Wang, Hang Zhou, Xiaokang Chen, Dongliang He, Tianshu Hu, Jingtuo Liu, Gang Zeng, and Jingdong Wang. Real-time neural radiance talking portrait synthesis via audio-spatial decomposition. *arXiv preprint arXiv:2211.12368*, 2022.
- [79] Justus Thies, Michael Zollhöfer, and Matthias Nießner. Deferred neural rendering: image synthesis using neural textures. *ACM Trans. Graph.*, 38(4):1–12, 2019.
- [80] Justus Thies, Mohamed Elgharib, Ayush Tewari, Christian Theobalt, and Matthias Nießner. Neural voice puppetry: Audio-driven facial reenactment. *Eur. Conf. Comput. Vis.*, 2020.
- [81] Aaron van den Oord, Yazhe Li, and Oriol Vinyals. Representation learning with contrastive predictive coding. *arXiv:1807.03748*, 2019.
- [82] Ashish Vaswani, Noam Shazeer, Niki Parmar, Jakob Uszkoreit, Llion Jones, Aidan N Gomez, Łukasz Kaiser, and Illia Polosukhin. Attention is all you need. In *Adv. Neural Inform. Process. Syst.*, 2017.
- [83] Konstantinos Vougioukas, Stavros Petridis, and Maja Pantic. End-to-end speech-driven realistic facial animation with temporal gans. In *IEEE Conf. Comput. Vis. Pattern Recog. Worksh.*, 2019.
- [84] Duomin Wang, Yu Deng, Zixin Yin, Heung-Yeung Shum, and Baoyuan Wang. Progressive disentangled representation learning for fine-grained controllable talking head synthesis. In *IEEE Conf. Comput. Vis. Pattern Recog.*, 2023.
- [85] Jiadong Wang, Xinyuan Qian, Malu Zhang, Robby T. Tan, and Haizhou Li. Seeing what you said: Talking face generation guided by a lip reading expert. In *IEEE Conf. Comput. Vis. Pattern Recog.*, 2023.
- [86] Kaisiyuan Wang, Qianyi Wu, Linsen Song, Zhuoqian Yang, Wayne Wu, Chen Qian, Ran He, Yu Qiao, and Chen Change Loy. Mead: A large-scale audio-visual dataset for emotional talking-face generation. In *Eur. Conf. Comput. Vis.*, 2020.
- [87] Zhou Wang, A.C. Bovik, H.R. Sheikh, and E.P. Simoncelli. Image quality assessment: from error visibility to structural similarity. *IEEE Trans. Image Process.*, 13(4):600–612, 2004.
- [88] Yuxiang Wei, Yupeng Shi, Xiao Liu, Zhilong Ji, Yuan Gao, Zhongqin Wu, and Wang-meng Zuo. Orthogonal jacobian regularization for unsupervised disentanglement in image generation. In *Int. Conf. Comput. Vis.*, 2021.
- [89] Xiuzhe Wu, Pengfei Hu, Yang Wu, Xiaoyang Lyu, Yan-Pei Cao, Ying Shan, Wen-ming Yang, Zhongqian Sun, and Xiaojuan Qi. Speech2lip: High-fidelity speech to lip generation by learning from a short video. In *Int. Conf. Comput. Vis.*, 2023.
- [90] Yibo Xia, Lizhen Wang, Xiang Deng, Xiaoyan Luo, and Yebin Liu. Gmtalker: Gaussian mixture based emotional talking video portraits. *arXiv:2312.07669*, 2023.
- [91] Wenqi Xian, Jia-Bin Huang, Johannes Kopf, and Changil Kim. Space-time neural irradiance fields for free-viewpoint video. In *IEEE Conf. Comput. Vis. Pattern Recog.*, 2021.

- [92] Yuelang Xu, Hongwen Zhang, Lizhen Wang, Xiaochen Zhao, Han Huang, Guojun Qi, and Yebin Liu. Latentavatar: Learning latent expression code for expressive neural head avatar. In *ACM Proc. SIGGRAPH*, 2023.
- [93] Shunyu Yao, RuiZhe Zhong, Yichao Yan, Guangtao Zhai, and Xiaokang Yang. Dfannerf: Personalized talking head generation via disentangled face attributes neural rendering. *arXiv preprint arXiv:2201.00791*, 2022.
- [94] Zhenhui Ye, Jinzheng He, Ziyue Jiang, Rongjie Huang, Jiawei Huang, Jinglin Liu, Yi Ren, Xiang Yin, Zejun Ma, and Zhou Zhao. Geneface++: Generalized and stable real-time audio-driven 3d talking face generation. *arXiv preprint arXiv:2305.00787*, 2023.
- [95] Zhenhui Ye, Ziyue Jiang, Yi Ren, Jinglin Liu, Jinzheng He, and Zhou Zhao. Geneface: Generalized and high-fidelity audio-driven 3d talking face synthesis. In *Int. Conf. Learn. Represent.*, 2023.
- [96] Richard Zhang, Phillip Isola, Alexei A Efros, Eli Shechtman, and Oliver Wang. The unreasonable effectiveness of deep features as a perceptual metric. In *IEEE Conf. Comput. Vis. Pattern Recog.*, 2018.
- [97] Hang Zhou, Yu Liu, Ziwei Liu, Ping Luo, and Xiaogang Wang. Talking face generation by adversarially disentangled audio-visual representation. In *Proc. AAAI Conf. Art. Intel. and Innov. App. Art. Intel. Conf. and AAAI Symp. Edu. Adv. Art. Intel.*, 2019.
- [98] Hang Zhou, Yasheng Sun, Wayne Wu, Chen Change Loy, Xiaogang Wang, and Ziwei Liu. Pose-controllable talking face generation by implicitly modularized audio-visual representation. In *IEEE Conf. Comput. Vis. Pattern Recog.*, 2021.
- [99] Yang Zhou, Xintong Han, Eli Shechtman, Jose Echevarria, Evangelos Kalogerakis, and Dingzeyu Li. Makelttalk: speaker-aware talking-head animation. *ACM Trans. Graph.*, 39(6):1–15, 2020.
- [100] Zheng Zhu, Guan Huang, Jiankang Deng, Yun Ye, Junjie Huang, Xinze Chen, Jiagang Zhu, Tian Yang, Jiwen Lu, Dalong Du, and Jie Zhou. Webface260m: A benchmark unveiling the power of million-scale deep face recognition. In *IEEE Conf. Comput. Vis. Pattern Recog.*, 2021.

Supplementary

Contents

The supplementary is organized as follows:

1. Additional Ablation Study in Sec. 6
2. Additional Results in Sec. 7
3. Implementation Details in Sec. 8
4. Discussion: Limitations and Ethical Considerations in Sec. 9

We strongly encourage the readers to watch our supplementary video.

6 Additional Ablation Study

Audio Encoder Learning. We conduct an ablation study on the impact of the self-supervised audio encoder learning. We find that our proposed audio representation improves the lip-sync performance. We show this impact in Figure 6(b), where the method with self-supervised audio encoder learning has better lip-sync performance than the method without it. We conduct this experiment without including expression input. Figure 6(a) illustrates the performance of our audio encoder learning qualitatively. Our proposed self-supervised learning leads to more accurate mouth shapes, corresponding to the spoken phonemes. Note that we omit the expression disentanglement during this evaluation and evaluate it on Obama2 and John Oliver from the datasets collected in LSP [56] and the PATS dataset [0, 51].

Interpreting Learnt Features. In Figure 7, we provide additional examples of interpolation between two expression features, learned by our expression transformer and representing two different emotions. As shown, our method learns semantically grounded features. In Figure 8, we demonstrate t-SNE plots of the expression features learned by our proposed transformer for two identities. The plots indicate that the learned features are well-behaved and clustered together according to the corresponding emotion annotations.

7 Additional Results

In Figures 9, 10, 11 we show additional results of rendered frames in comparison with state-of-the-art methods for expression and audio-driven talking face generation (EAMM [43] and PD-FGC [84]), categorical emotion based talking face generation (EAT [28]) as well as the audio-only AD-NeRF [36], and expression-only NeRFace [27]. We also compare with Our method outperforms all the other methods, transferring the expression and audio inputs with a high fidelity, while preserving the target identity.

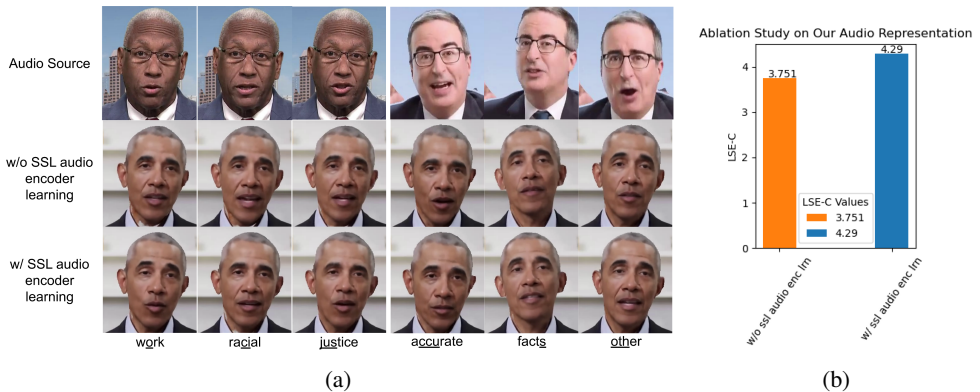


Figure 6: (a) illustrates the ablation with and without self-supervised audio encoder learning. Our audio encoder learning produces better and more accurate mouth shapes as compared to without it. In (b) we quantitatively evaluate our method without and with self-supervised audio encoder learning.

8 Implementation Details

8.1 Landmark Autoencoder

8.1.1 Dataset

For this task, we use the complete available set of frontal view MEAD [46] dataset videos, *i.e.* “part0”. 39 identities from the dataset were kept for training and rest 9 for validation. We used 68 point landmarks of which 17 landmarks corresponding to the face contour were discarded for training the landmark autoencoder and these were input to the autoencoder as arrays. We extract landmarks from square frame of 480×480 rescaled and cropped from the initial resolution of 1920×1080 (by cropping the middle 1080×1080 frame from the video and then resizing it to 480×480).

8.1.2 Pipeline

The landmark encoder and decoder consisted of 4 MLPs each with 256, 256, 128 as the hidden layer sizes and Leaky ReLU activations (negative slope set to 0.02). The output features e_f and e_m were 64 dimensions each. For swapping, ϵ was set to 0.8 and the last 20 points in the landmarks representing the lips were used.

We noticed that sampling the frames A and B from different videos of different identities or emotions would encourage the network to learn features that may contain identity and emotion information. Essentially, the network would try to differentiate between identity-specific or emotion-specific characteristics of the face, rather than learn lip motion features. This would deteriorate the performance of our dynamic NeRF, which requires conditioning on a powerful audio representation. Thus, we sample frames A and B randomly from the same video of an identity.

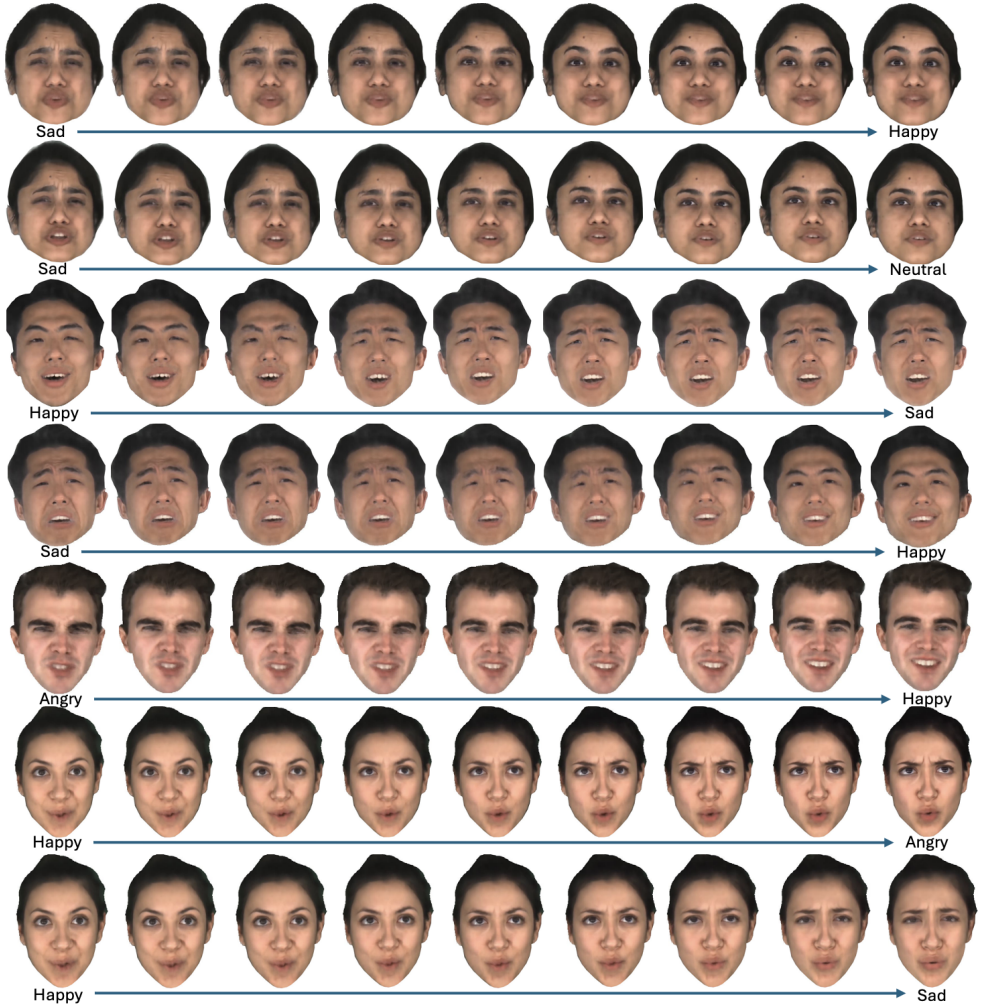


Figure 7: Additional analysis that shows that the expression encoder disentangles features that are semantically grounded and well-behaved. Interpolation of features from left to right leads to semantically meaningful expressions.

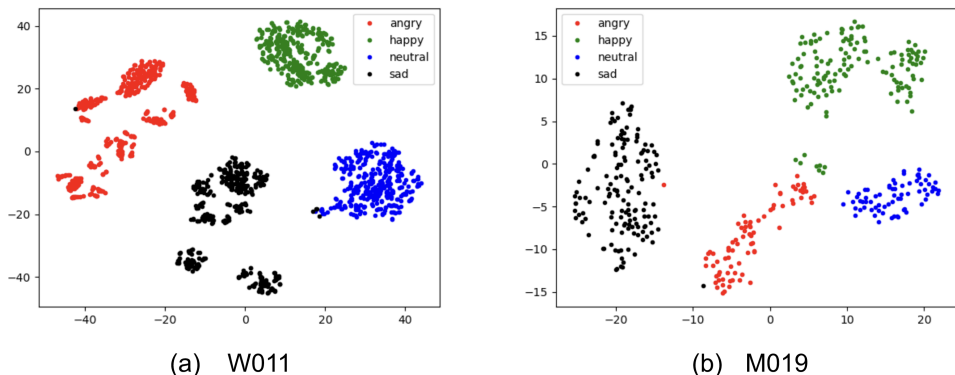


Figure 8: t-SNE plots of the expression features learned by our expression transformer for the “W011” and “M019” identities of MEAD.

8.1.3 Training

The model was optimized using Adam [43] with default parameters and 10^{-5} as weight decay value. We trained the landmark encoder for 15 epochs on a single Nvidia V100 GPU with a batch size of 256 which takes ≈ 12 hours.

8.2 Contrastive Learning

8.2.1 Dataset

For this task, the complete available set of frontal view videos from MEAD dataset was used, *i.e.* from “part0”. We use the same splits used for training the landmark autoencoder, *i.e.* 39 identities for training and rest 9 for validation. We extract landmarks from square frame of 480×480 rescaled and cropped from the original resolution of 1920×1080 (by cropping the middle 1080×1080 frame from the video and then resizing it to 480×480). The corresponding audio signals for each video was converted into DeepSpeech [2] features.

8.2.2 Pipeline

We use the trained encoder from our Landmark Autoencoder and keep its weights frozen during training. We use the same architecture as the audio encoder of [36] for our audio encoder. During training, negative audio samples were randomly selected from the same identity but different video. Further, the temperature τ in the InfoNCE loss formulation in Eq. 2 was set to 0.1.

8.2.3 Training

The audio encoder was optimized using Adam with learning rate set to 10^{-3} and default parameters for the rest with an exponential decay and final learning rate to be 5×10^{-6} . We trained this model for 30 epochs on a single Nvidia V100 GPU with a batch size of 256 which takes ≈ 2 hours.

8.3 Expression Transformer

8.3.1 Dataset

We use the MEAD dataset as it contains identities speaking the same utterances in different emotions. This dataset is not consistent in the sentences that are spoken in different emotions and hence only videos of an utterance with corresponding videos of the same utterance present in other emotions are used to train the expression transformer. This filtering leads to 18 unique sentences for each identity. For each identity from MEAD that was used to test in our method, 60 pairs of videos where each video in the pair speak the same sentence with different emotions were used for training. The rest (15 – 24) of the pairs of videos formed the validation set. Note that we only included the highest level videos of the emotions “angry”, “happy” and “sad”, and the only level of “neutral” for these pairs.

For each video in these pairs, we extract the emotion features e_{emo} per video frame, using a vanilla ResNet50-based emotion recognition network from [17] trained on AffectNet [58] on expression classification, valence, and arousal regression task jointly. We use the features from the ResNet backbone before being processed by any classification/regression heads. To account for any misalignment of the utterances of different emotions, we incorporate the dynamic time-warping (DTW) algorithm [9] to align the input emotion feature sequences.

8.3.2 Pipeline

We find that each person’s style of speaking with a particular emotion is unique, so training a separate expression encoder is necessary. For the expression autoencoder, we used a transformer architecture with linear layers in the beginning to map down the 2048 dimensional emotion recognition features to 128 via two MLP layers with Leaky ReLU activation and a hidden layer size of 512. The output of the encoder is split in half resulting in 64 dimension features for lip motion and expressions. The encoder had 8 attention heads, 3 layers with dropout enabled and set to 0.2. A positional encoding was applied similar to [12] and since a decoder was used, the input sequence was padded with start and end sequence vectors. The expression decoder had the same architecture in terms of the number of attention heads and layers. The start and end sequence tokens were stripped off and the features were mapped back to 2048 dimensions using a 2 layer MLP with Leaky ReLU activations (negative slope set to 0.02) and hidden layer size of 512. ω is set to 8. Further, δ is set to 0.8. During training, all features output from the encoder corresponding to each input feature are passed through to the decoder after the swapping operation.

8.3.3 Training

The expression transformer was optimized using Adam with default parameters and weight decay of 10^{-5} . We trained this model for 20 epochs on a single Nvidia V100 GPU with a batch size of 256 which takes \approx 1 hour.

8.4 NeRF

8.4.1 Dataset

We used identities from MEAD to train the NeRF. For each identity, we used the highest level emotions videos of “angry”, “happy” and “sad”, and the only level of “neutral” to train

the NeRF. Since videos in MEAD are only 4-8 seconds long which are impractically small videos for training NeRFs, we concatenate different videos of the same emotion. Further, all videos in the same emotion of one identity were not captured in the same pose or at the same distance from the camera. To ensure that the NeRF is not overfitted to specific emotion - head pose or emotion - camera distance pairs, we filter the videos of each identity. More specifically, videos of an identity were filtered on the basis of three factors: (1) whether they were shot immediately following each other (determined by the lack of sudden change in pose and distance from camera if two videos were concatenated), (2) whether the determined focal length for the face after fitting a 3DMM [14, 52] was the same, and (3) whether the pose distribution were very similar. After concatenation, each video of a particular emotion was ≈ 15 seconds long.

8.4.2 Pipeline

The talking head is represented by an implicit function F_{Θ} that corresponds to an MLP. The model architecture for this implicit function is the same as AD-NeRF, consisting of 8 linear layers with a hidden size of 128 and ReLU activations. However, the input size was changed from 32 (audio features only) to 96 (audio features + expression features). For each video frame, we fit a 3DMM [14, 52] and extract the head pose and camera parameters, in order to estimate the viewing direction \mathbf{d} . After converting the head pose from the observation space to the canonical space, we use the estimated head pose as the viewing direction \mathbf{d} of the radiance field. As in AD-NeRF, we positionally encode 3D point \mathbf{x} with 10 frequencies and viewing direction \mathbf{d} with 4 frequencies but not features e_e and e_a . While training the NeRF, the frames from videos of each emotion were randomly picked with their corresponding audio features e_a , expression features e_e (by spanning a window of features of size ω around the corresponding index and selecting the $\omega/2$ th feature of the output as e_e) and pose. Similar to AD-NeRF [56], we parse the head from the background using an automatic parsing method, namely MaskGAN [25]. Further, we assume that the last point of each ray takes the RGB color of the background and lies on it. During inference, we render the talking face on a white background.

8.4.3 Training

The NeRF was optimized using Adam with an initial learning rate 5×10^{-4} that decays exponentially to 5×10^{-5} . At each iteration, we randomly sample 2048 rays for a video frame. The model is trained for 400,000 iterations (around 2 days on a single GPU). We also enable the fine-tuning of the audio encoder during this training with a learning rate of 5×10^{-6} .

8.5 Metrics

We compute the visual quality metrics, namely PSNR, SSIM [87], LPIPS [96], after extracting a face bounding box using 3DDFA V2 [54, 85] and cropping the face. The target frame from the expression source is also cropped in the same manner and resized to the size of the cropped source frame. This is done so that the background is not included in the quality computation. The identity preservation metric (ACD) is measured using ArcFace [18], a ResNet50-based network trained on WebFace [100]. Specifically, we used “buffalo_1” model from the insightface repository [63]. For lip-sync confidence [65] of NeRFace, we compute

the metric of each video against all testing audio sources and report the average. Similarly, for Exp-Diff [84] for AD-NeRF, we compute the metric of a particular video against all testing expression source videos and report an average.

9 Discussion

9.1 Limitations

An important factor of our method is the 3DMM fitting that is used as ground truth to extract the head pose and camera parameters (see Sec. 3.3 of the main paper and Sec. 8.4.2). This fitting can be noisy and the error can be propagated to the final generated videos. Improving the face tracking further would be an interesting future work. In addition, we propose a NeRF-based representation that synthesizes high-quality expressive talking faces. We believe that our proposed audio and expression representations can be easily extended to other neural rendering pipelines, like 3D Gaussian Splatting [44] that provides faster training and inference times. We plan to explore this direction in the future.

9.2 Ethical Considerations

We would like to note the potential misuse of generation methods. With the rise of “deep fakes”, it becomes easier to make photorealistic fake videos of any speaker. These can be used for malicious purposes, e.g. to spread misinformation. To this end, it is important to develop accurate methods for fake content detection and forensics [10, 69]. We intend to share our source code to help improving such research. In addition, appropriate procedures must be followed to ensure fair and safe use of videos if used for training or inference. In our work, we use MEAD that is a publicly available dataset, featuring actors talking with different emotions in a controlled setup and has been used by several other published works.

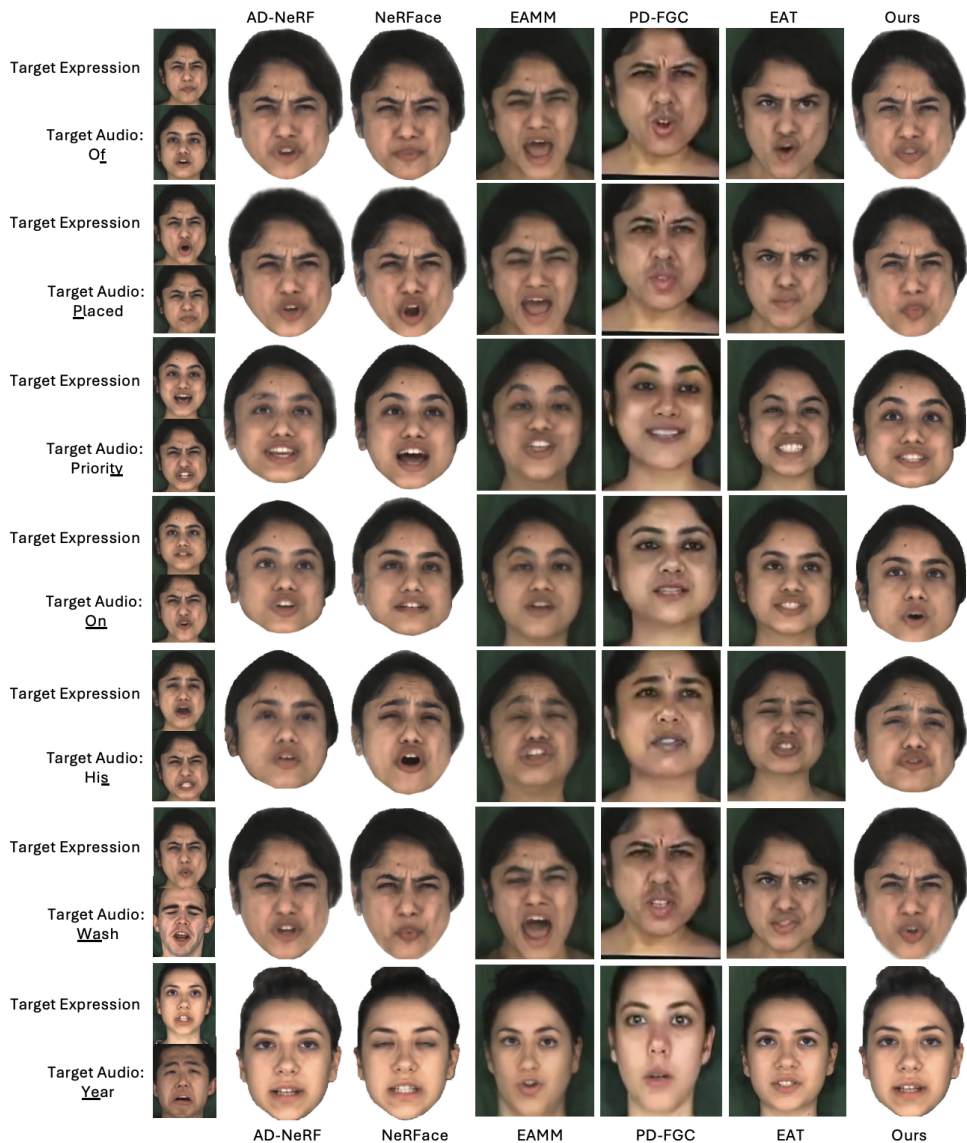


Figure 9: Talking face generation guided by target expression and audio (1st column) compared with the state-of-the-art.

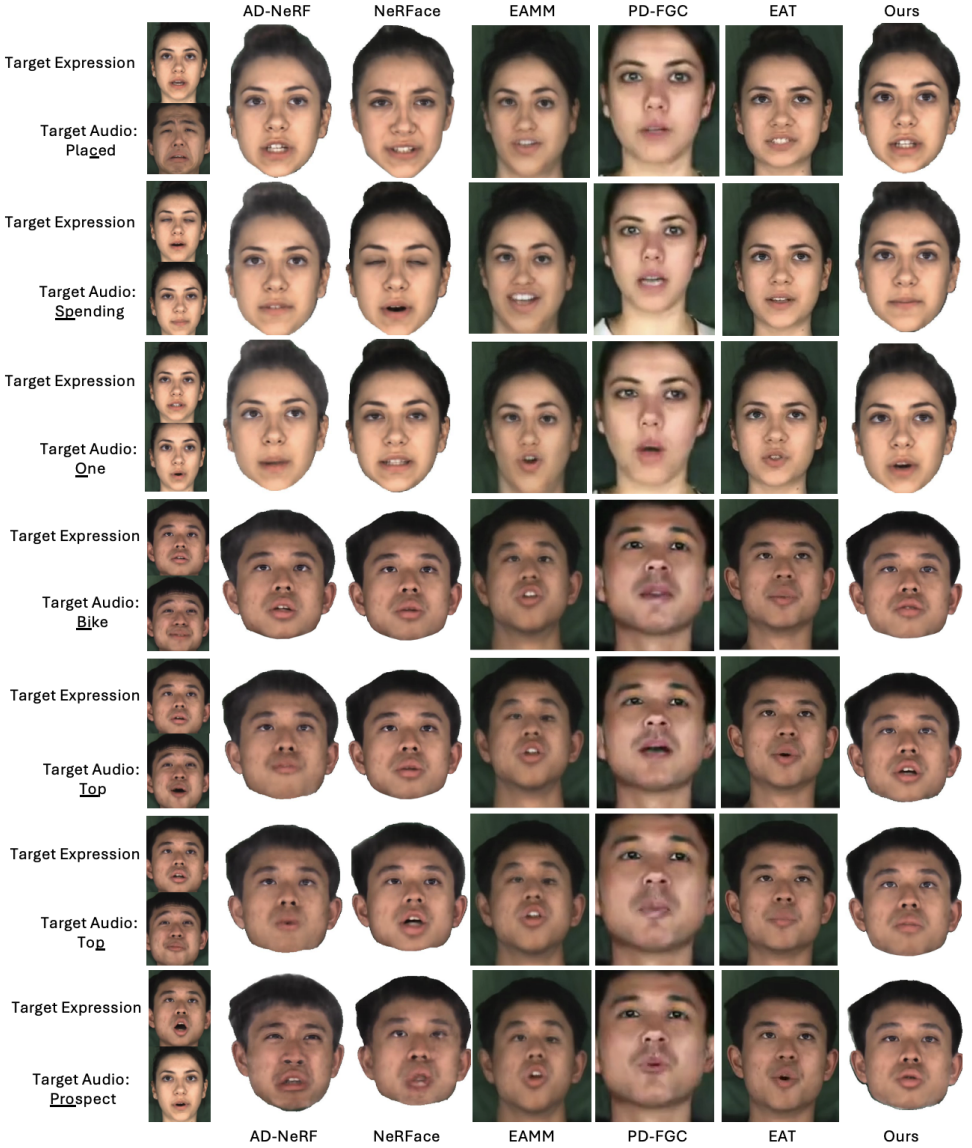


Figure 10: Talking face generation guided by target expression and audio (1st column) compared with the state-of-the-art.

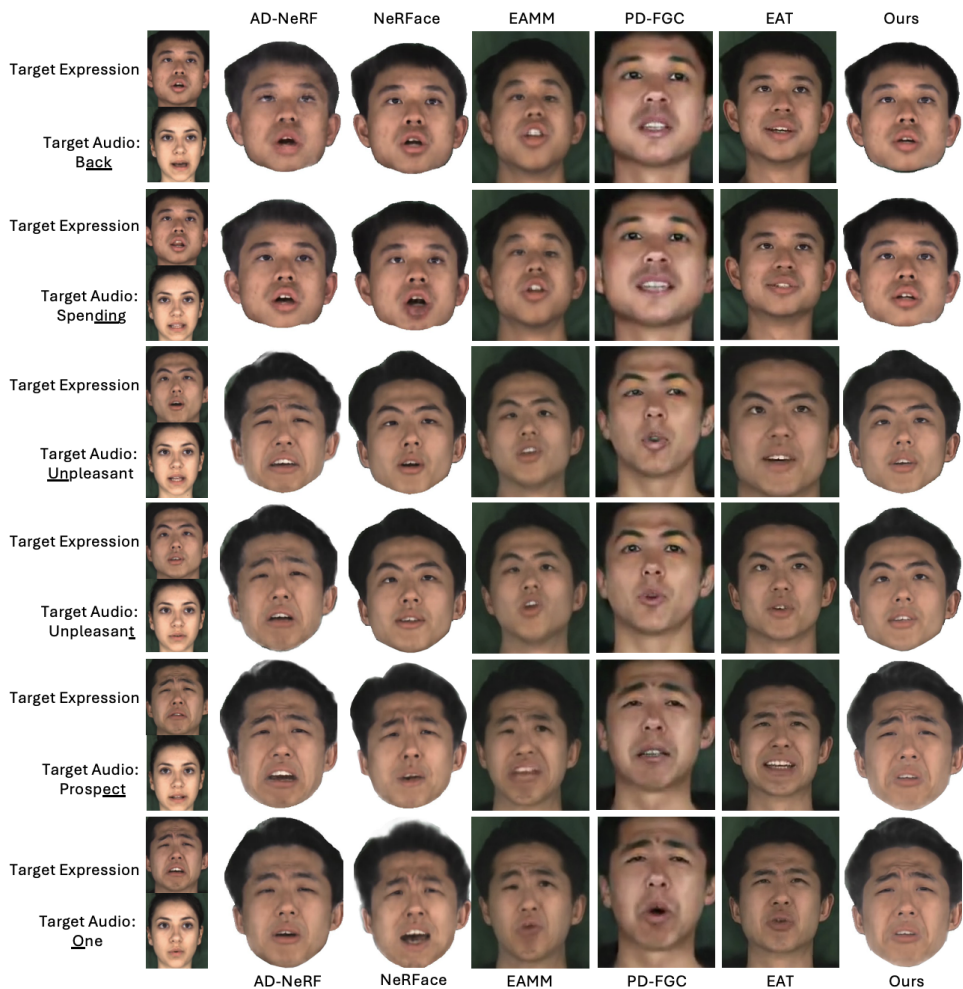


Figure 11: Talking face generation guided by target expression and audio (1st column) compared with the state-of-the-art.